applied sciences

MDPI

Article

Global Maximum Power Point Tracking of a Photovoltaic Module Array Based on Modified Cat Swarm Optimization

Kuei-Hsiang Chao * and Thi Bao-Ngoc Nguyen

Department of Electrical Engineering, National Chin-Yi University of Technology, Taichung 41170, Taiwan; nguyenthibaongoc.2000a@gmail.com

* Correspondence: chaokh@ncut.edu.tw; Tel.: +886-4-2392-4505 (ext. 7272); Fax: +886-4-2392-2156

Abstract: The main purpose of this study was to research and develop maximum power point tracking (MPPT) of a photovoltaic module array (PVMA) with partial module shading and sudden changes in solar irradiance. Modified cat swarm optimization (MCSO) was adopted to track the global maximum power point (GMPP) of the PVMA. Upon a sudden changes in solar irradiance or when certain modules in the PVMA were shaded, the maximum power point (MPP) of the PVMA will change accordingly, and multiple peak values may appear on the power–voltage (P-V) characteristic curve. Therefore, if the tracking pace is constant, the time required to track the MPP might extend, and under certain circumstances, the GMPP might not be tracked, as only the local maximum power point (LMPP) can be tracked. To prevent this problem, a maximum power point tracker based on MCSO is proposed in this paper in order to adjust the tracking pace along with the slope of the P-V characteristic curve and the inertia weight of the iteration formula. The initial voltage for tracking commencement was set to 0.8 times the voltage at the maximum power point of the PVMA under standard test conditions. Firstly, MATLAB 2022a was used to construct the four-series, three-parallel PVMA model under zero shading and partial shading. The feedback of PVMA voltage and current was obtained, where the GMPP was tracked with MCSO. From the simulation results, it was proven that, under different shading percentages and sudden changes in solar irradiance for partial modules in the PVMA, the MCSO proposed in this paper provided better tracking speed, dynamic response, and steady performance compared to the conventional CSO.

Keywords: modified cat swarm optimization; partial shading; photovoltaic module array; maximum power point tracking; global maximum power point; local maximum power point; tracking speed; dynamic response and steady performance

Citation: Chao, K.-H.; Nguyen, T.B.-N. Global Maximum Power Point Tracking of a Photovoltaic Module Array Based on Modified Cat Swarm Optimization. *Appl. Sci.* **2024**, *14*, 2853. https://doi.org/10.3390/app14072853

Academic Editors: Manuela Sechilariu, Saleh Cheikh-Mohamad and Berk Celik

Received: 3 January 2024
Revised: 6 March 2024
Accepted: 15 March 2024
Published: 28 March 2024

1. Introduction

Solar energy is a source of renewable energy, and a PVMA can convert it into electrical power available for use. Since the process of photovoltaic power generation releases hardly any greenhouse gases (GHGs) or other contaminants, the environmental impact is quite limited, which helps in mitigating global climate change as well as reducing air and water contamination. Therefore, solar energy has become an ideal source of alternative energy in recent years [1,2]. In a photovoltaic power generation system, if the PVMA connects to the load directly, the output power of the module array is determined by the load; thus, the output power of the PVMA cannot reach the maximum value. The output characteristic curve of the PVMA is determined by the temperature and solar irradiance [3]; the two continuously change over time. Therefore, to enhance the power generation efficiency of the PVMA, an MPPT controller must be used. At present, common and conventional MPPT methods include the constant voltage method (CVM) [4–6], the power feedback method (PFM) [7,8] and the perturb and observe method (P&O) [9–11].

A continuous change in solar irradiance and the appearance of shade will have an impact on the characteristic curve of the PVMA, and these factors could generate multiple

peak values on the P-V characteristic curve [12], which could lead to failure of tracking the GMPP with the conventional MPPT method; thus, the power loss is increased and the conversion efficiency is reduced. To solve the problem of multiple peak values on the P-V characteristic curve, experts and scholars have proposed many smart MPPT methods in recent years [13]. The objective of these methods is to achieve higher power generation efficiency of a PVMA in circumstances of unstable solar irradiance and multiple peak values. The most common smart algorithms include particle swarm optimization (PSO) [14], firefly algorithm (FA) [15–17], grey wolf optimization (GWO) [18,19], artificial bee colony (ABC) [20], and cat swarm optimization (CSO) [21]. Among them, PSO [14] is an optimization algorithm based on swarm intelligence inspired by the collective behavior of social organisms such as birds or fish in nature. Usually, PSO is implemented to solve the problem of value optimization, which enables the allocation of the global maximum value of one target function. The fundamental concept of PSO is to search for the optimum by simulating the movement of a particle (also referred to as an individual) in the search space using collaboration. Compared to other algorithms, PSO is simpler and requires fewer evolution swarms. However, PSO needs to be set with adequate initial parameters, such as particle quantity and speed range, and incorrect parameter setting might lead to a longer duration for tracking the GMPP.

FA [15–17], an optimization algorithm of swarm intelligence that was proposed by Xin-She Yang at Cambridge University in 2008, was inspired by the flickering behavior of fireflies in nature. The algorithm mimics the behavior of fireflies in terms of mutual attraction via flashing signals. In this algorithm, the luminance of fireflies is directly proportional to the level of attraction: fireflies with higher luminance generate a greater attraction for nearby fireflies. When the luminance becomes the same, the fireflies move randomly; thus, the brightest firefly will be the optimum. The advantages of FA include fewer parameters, a more extensive range for searching, fast convergence, and more stable performance, while the disadvantage is that this algorithm might be stuck tracking the LMPP when its function has multiple peak values.

GWO [18,19], an inspired optimization algorithm based on the social behavior of grey wolves in nature, has been extensively applied to track the GMPP of a PVMA. The objective is to search for the optimal target, which means tracking the MPP of the PVMA. By simulating the collaboration and leading behavior of grey wolves, the algorithm can track the MPP at a certain moment. Usually, the converging speed of GWO is relatively slower, especially when multiple peak values appear on the P-V characteristic curve, which might cause difficulty for the system in swiftly tracking the GMPP under conditions of fast changes in irradiance.

ABC [20] is a global optimization algorithm that is a type of swarm intelligence algorithm. This algorithm was proposed by Dervis Karaboga in 2005, and the inspiration came from the honey-harvesting behavior of bee colonies. Based on the different roles of bees in the colony, bees in the algorithm, through information sharing and interactions, collaborate to search for the optimum. The advantages of this algorithm include high stability, fewer control parameters, and easier comprehension, while the disadvantage is the problem of premature convergence. Therefore, it might lead to similar results to the algorithm mentioned above, where the true MPP might not be able to be tracked.

CSO, a global optimization algorithm that originated from the characteristic behavior of cats, was first proposed by S. C. Chu, P. W. Tsai, and J. S. Pan in 2006 [21]. This algorithm is also a swarm intelligence algorithm. It is a method of addressing complex optimization problems using a combination of cat behaviors: seeking and tracking. However, the disadvantages of CSO are similar to those of the algorithms mentioned above. Since the algorithm includes seeking and tracking modes, it can result in slower convergence if inadequate parameters are selected, where the GMPP cannot be tracked.

To address the disadvantages of various conventional and smart MPPT methods, MCSO is proposed in this paper for the MPPT of a PVMA. First, the characteristic curve of the photovoltaic module array is simulated in the MATLAB 2022a software, and the theory

of MCSO is described, which is used to carry out the maximum power point tracking test for the photovoltaic module array. Finally, it is proven from the simulation results that the proposed MCSO method does improve upon the shortcomings of the conventional CSO method.

2. PVMA Output Characteristics under Different Shading Conditions

Since the output characteristic curve of a PVMA is non-linear, the output power is affected by the solar irradiance, ambient temperature, and shading condition under different series–parallel configurations; thus, the P-V and I-V characteristic curves under the same ambient temperature will display multiple peak values along with the change in solar irradiance and shading of partial modules.

In this paper, SWM20W photovoltaic modules produced by MPPTSun Co., Ltd. (Dongguan, China) [22] were used to assemble the PVMA, and the electrical performance parameters of a single module are shown in Table 1. First, the MATLAB software was utilized to build the model of a single photovoltaic module, which was then assembled into the 4-series, 3-parallel PVMA for conducting tests. The I-V and P-V characteristic curves derived from module simulation at a temperature of 25 °C and different irradiance levels are shown in Figure 1.

Table 1. Specifications of electrical performance parameters for SWM20W photovoltaic modules made by MPPTSun [22].

Parameter	Value
Maximum output power (P_{max})	20 W
Current of maximum output power (I_{mpp})	1.1 A
Voltage of maximum output power (V_{mpp})	18.18 V
Short-circuit current (I_{sc})	1.15 A
Open-circuit voltage (V_{oc})	22.32 V
Overall dimensions of single module	395 × 345 × 17 mm

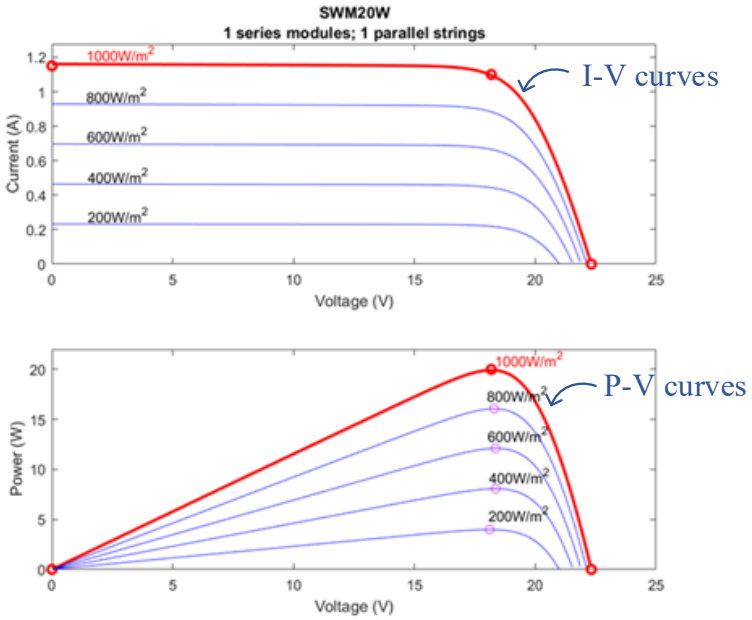

Figure 1. I-V and P-V characteristic curves derived from module simulation at 25 °C and different irradiance levels.

3. Conventional Cat Swarm Optimization

Cat swarm optimization (CSO) is a global optimization algorithm based on cat behavior that was first proposed by Chu et al. in 2006 [21]. CSO mimics two cat behaviors,

seeking and tracking, to solve optimization problems; thus, it includes a seeking mode and a tracking mode. The seeking mode simulates the state of a cat relaxing and looking around, while the tracking mode simulates a cat tracking a target. A flowchart of conventional CSO is shown in Figure 2.

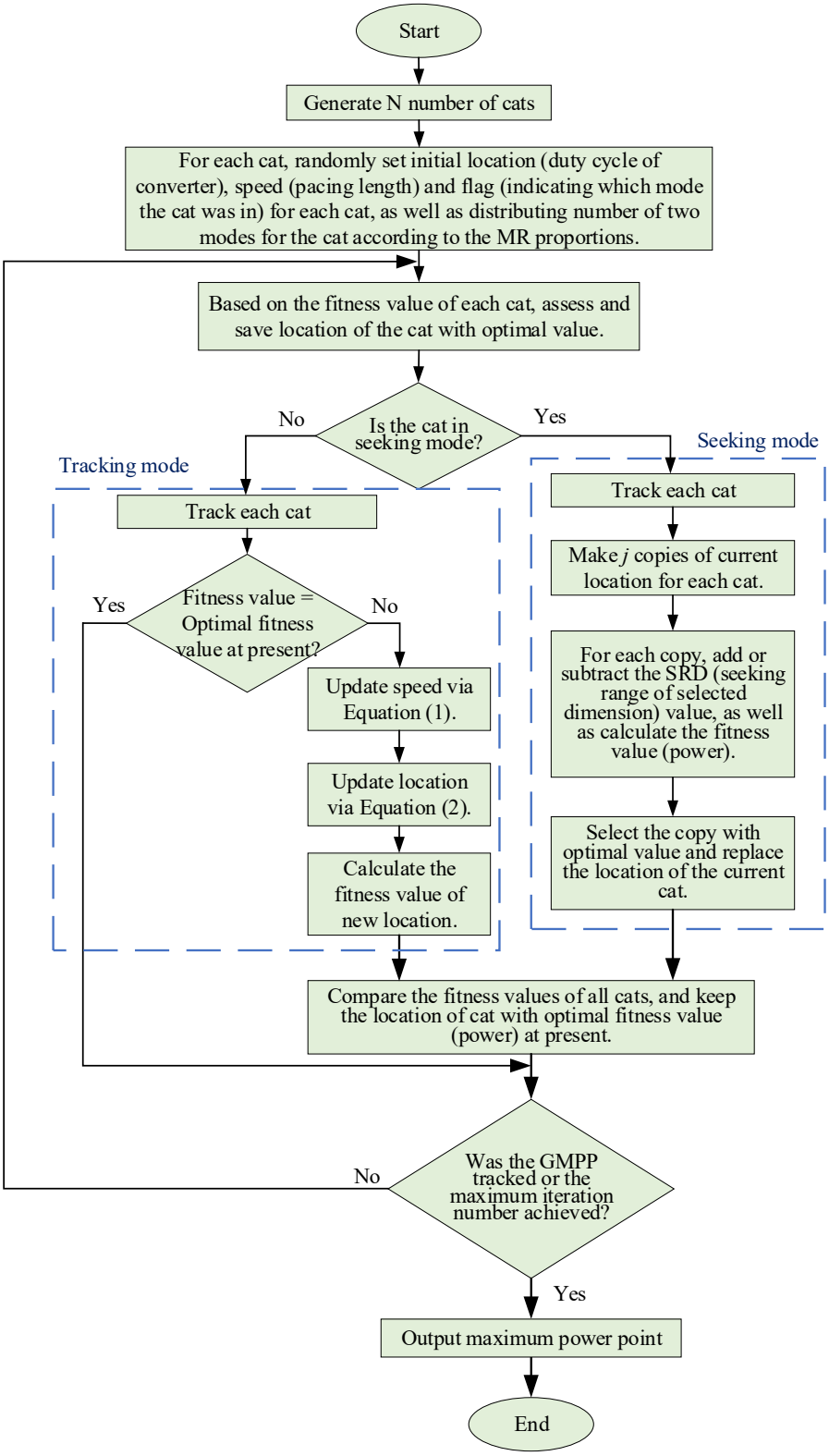

Figure 2. Flowchart of conventional CSO.

First, the method requires initialization and the setting of certain parameters, including the quantity of cats, the maximum number of iterations, and the initial location, speed, and flag of each cat. The parameters are described as follows:

- Cat quantity: This ensures the number of cats needed for the algorithm, which affects the converging capability and speed of CSO. In this study, we used 6 cats.
- Initial location (duty cycle of converter): The initial location of each cat should be set right from the start; in this study, they were set randomly.
- Speed (tracking pace): After setting the initial location, the initial speed can be calculated accordingly.
- Cat flag: This parameter refers to the Boolean value indicated with only "yes" or "no". "Yes" means that the cat is in seeking mode and "no" means that the cat is in tracking mode.
- Maximum number of iterations: The condition for iteration termination was set here to ensure that the CSO operation would cease within a certain time frame.

In step 1, the current fitness value (i.e., currently tracked power value) for each cat was allocated at the current location and the fitness value was assessed, and the location (x_{best}) of the cat with the optimal fitness value was saved. In CSO, the cats are assigned to different modes according to the set mixture ratio (MR). The MR represents the proportion of cats distributed to tracking mode, and has a value between 0 and 1. In the program, the MR was often set with smaller numbers. For example, if 10 cats were utilized in CSO with an MR of 0.2, 2 cats would be assigned to tracking mode and 8 cats would be assigned to seeking mode. The flag for cats assigned to seeking mode would be set as "yes", and the main task of seeking mode is to update the cat location. The flowchart of CSO in Figure 2 describes seeking and tracking modes on the left and right sides, respectively.

Once the cats were assigned to the two work modes, each cat performed the task of seeking or tracking in the current location with the optimal fitness value. Subsequently, the fitness value of the individual allocated location was compared with the current optimal fitness value. If the two values were unequal, the program continued to seek and track, so better fitness values could be allocated. However, if the two values were equal, the program would be checked for compliance with the terminating condition: the maximum iteration number. If the maximum iteration number was reached, the program ceased to operate. Conversely, if the maximum iteration number was not reached, the program continued to operate. Since the iteration number set in this study was relatively small at 30, the program did not cause slower tracking speed due to excessive iterations.

3.1. Seeking Mode

In seeking mode, all cats with a "yes" flag enter seeking mode. First, each cat executes the "copy" action and the number of copies is denoted as j. This parameter can be set by the user. Consequently, the program adds or subtracts the seeking range of selected dimension (SRD) for cats. SRD is the movable distance of cats in front and rear locations. This parameter can be set by the user; in this study, it was set at 0.2%, and the SRD range was 0–100%. The execution of adding or subtracting SRD is determined by the work mode that can produce a better fitness value, and the fitness value (power) in the new location is then calculated. Finally, the program selects the location of the cat with the optimal fitness value, which is used to replace the location of the current cat.

3.2. Tracking Mode

Cats with a "no" flag enter tracking mode. First, the fitness value (current power value) of each cat is determined based on whether it is equal to the current optimal fitness value (optimal power value). For cats with a "yes" flag, the program is checked for compliance with the terminating condition (whether the maximum iteration number has been reached). If the terminating condition is not met, each cat continues to be executed with the following steps:

1. Update tracking speed v_i according to Equation (1):

$$v_i(t+1) = v_i(t) + r^* c^* [x_{best}(t) - x_i(t)] \quad (1)$$

where t is the current iteration number (t = 1–30); $v_i(t+1)$ is the tracking speed of cat i after update; $v_i(t)$ is the tracking speed of cat i before update; r is a random number between 0 and 1; c is the speed coefficient (set at a constant value of 1.4 in conventional CSO); x_{best} is the location of the cat with the current optimal fitness value; and x_i is the location of cat i with the current optimal fitness value.

2. Update cat location x_i according to Equation (2):

$$x_i(t+1) = x_i(t) + v_i(t+1) \quad (2)$$

where $x_i(t+1)$ is the location of cat i after update; x_i is the location of cat i before update; $v_i(t+1)$ is the tracking speed of cat i after update; and t is the current iteration number (t = 1–30).

After updating the speed and location, the current fitness values of each cat and seeking mode are compared, and the location of the cat with the current optimal fitness value is kept.

4. Proposed MCSO

To improve the tracking speed response and steady performance of the conventional CSO, MSCO is proposed in this paper. The method includes an initial tracking voltage fixed at 0.8 times the MPP voltage under STC, combined with the slope of the P-V characteristic curve and inertial weight to adjust the tracking pace.

4.1. MCSO with Fixed Initial Tracking Voltage

Although the P-V characteristic curve of the PVMA will change under different solar irradiance levels or the partial shading of modules, it can be observed from Figure 3 that upon a sudden change in solar irradiance (from 1000 to 500 W/m^2), there was no extensive difference in MPP voltage. To improve the tracking speed of the conventional CSO, the initial tracking voltage V_{begin} was first fixed at 0.8 times the MPP voltage V_{mp} (i.e., V_{begin} = 0.8 V_{mp}). Therefore, each tracking would commence from V_{begin}. Despite the change in solar irradiance, the initial tracking voltage was approximately around the GMPP; therefore, this method can swiftly and steadily track the GMPP.

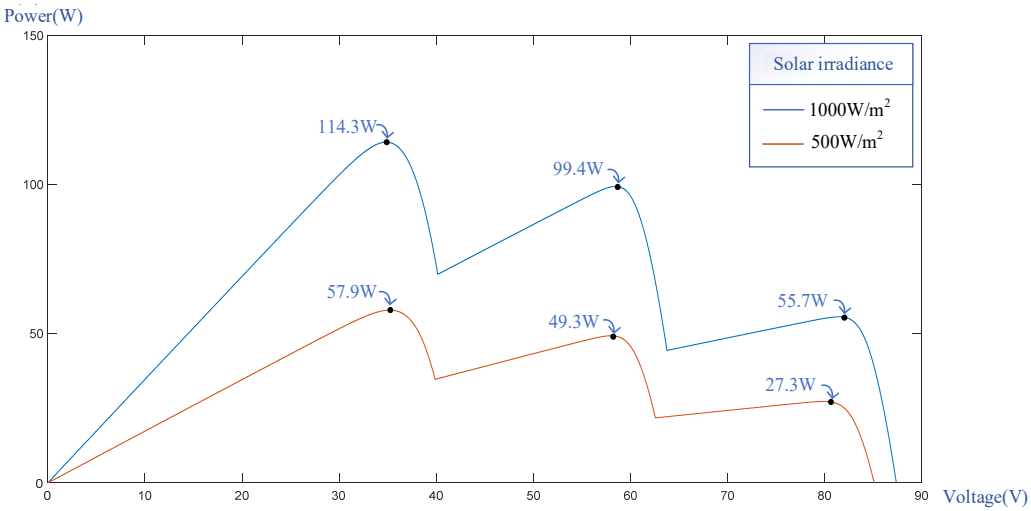

Figure 3. P-V characteristic curve upon sudden change in solar irradiance with partial module shading.

4.2. MCSO with Fixed Initial Tracking Voltage Combined with Tracking Pace Adjusted with Slope of P-V Curve

Although the MCSO with a fixed initial tracking voltage provided better tracking speed, it still used the same fixed tracking pace as the conventional CSO. Therefore, if the tracking pace is set to be excessively small, the tracking speed of the system will be affected. Conversely, if the tracking pace is set to be excessively large, although the tracking speed could increase, there will be a greater amplitude of oscillation when tracking in the vicinity of the MPP, where the tracking efficiency will be reduced.

To solve this problem and not affect the tracking speed at the same time, MCSO with a fixed initial tracking voltage was adopted in this study. In addition, the change intervals of the slope for the P-V characteristic curve in Table 2 were utilized to automatically adjust the speed coefficient (c) the MSCO in Equation (1). Therefore, the tracking pace could be adjusted to be smaller when the work point was close to the GMPP, which prevented excessive tracking oscillation and a loss of output power. Similarly, when the work voltage point was far away from the GMPP, the tracking pace could be increased to accelerate the tracking speed. This method of control could increase the tracking speed and reduce the oscillation amplitude near the MPP at the same time. Moreover, upon sudden changes in solar irradiance, the system could adjust the tracking pace instantly to realize fast and accurate MPPT.

Table 2. Adjustment relations between slope intervals of P-V characteristic curve and speed coefficient, c.

Slope Interval of P-V Characteristic Curve	Speed Coefficient (c) in Equation (1)
Interval m_1: $m > 2$	c = 1.4
Interval m_2: $2 > m \geq 1.3$	c = 1.3
Interval m_3: $1.3 > m \geq 0.8$	c = 1.2
Interval m_4: $0.8 > m \geq 0$	c = 1.1
Interval m_5: $0 > m \geq -1$	c = 1.0
Interval m_6: $m \leq -1$	c = 1.2

Figure 4 displays the adjustment relations between the slope of the P-V characteristic curve and speed coefficient (c) in Table 2 for the proposed MCSO, where m is the slope of the P-V characteristic curve. From Figure 4, the following can be observed:

(1) When slope m is less than zero, it indicates that the system has tracked to the right side of the MPP, and the tracking direction is heading toward the MPP at the left.
(2) When slope m is greater than zero, it indicates that the system has tracked to the left side of the MPP, and the tracking direction is heading toward the MPP at the right.
(3) When slope m is zero, it indicates that the system has tracked the MPP. The slope (m) and power variation (dP) are defined by Equations (3) and (4), respectively:

$$m = \frac{\mathrm{d}P}{\mathrm{d}V} = \frac{P_k - P_{k-1}}{V_k - V_{k-1}} \tag{3}$$

$$\mathrm{d}P = P_k - P_{k-1} \tag{4}$$

where P_k and V_k are the power and voltage values of the current operating point, respectively, and P_{k-1} and V_{k-1} are the power and voltage values of the previous operating point.

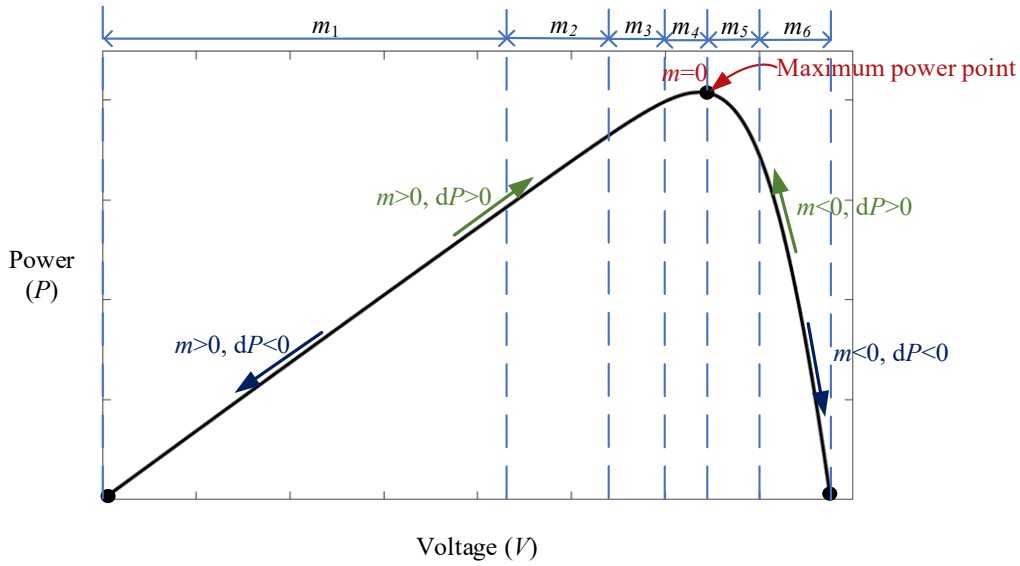

Figure 4. Interval division relations for parameters automatically adjusted according to slope of P-V characteristic curve under MCSO.

4.3. MCSO with Fixed Initial Tracking Voltage Combined with Tracking Pace Adjusted by Inertia Weight

In CSO, inertia weight is an important parameter. Since the selection and adjustment of inertia weight could have a significant effect on the tracking performance of the algorithm, minor adjustments to this parameter could affect the balance of the optimization process and lead to better tracking results. Therefore, the parameter of inertia weight was added to Equation (1) to update the CSO speed in this paper. In addition to fixing the initial tracking voltage at 0.8 V_{mp}, the learning rate was combined to adjust the tracking pace. The equation for updating the MCSO speed can be expressed as Equation (5):

$$v_i(t+1) = w^* v_i(t) + r^* c^* [x_{best}(t) - x_i(t)] \quad (5)$$

The values in Equation (5) can be used to adjust the inertia weight (w). The distance represents the difference between the optimal location found so far and the present location of each cat in CSO. Table 3 lists the adjustment relations between distance change $| x_{best}(t) - x_i(t) |$ and parameter w. When the distance is smaller, it indicates that the cat is already close to the MPP. For more accurate convergence at such a point and to reduce the oscillation amplitude of tracking back and forth, a smaller inertia weight (w) will be used. Conversely, if the distance is greater, it indicates that the cat is farther away from the GMPP. A greater inertia weight (w) will then be used to enhance the tracking speed. Therefore, in addition to increasing the tracking speed, it was possible to accurately work near the MPP to reduce power loss during the tracking process.

Table 3. Adjustment relations between distance change $| x_{best}(t) - x_i(t) |$ and inertia weight, w.

a= $\| x_{best}(t) - x_i(t) \|$	The Inertia Weight (w) in Equation (5)
$1 \geq a \geq 0.6$	$w = 0.4$
$0.6 > a \geq 0.5$	$w = 0.35$
$0.5 > a \geq 0.4$	$w = 0.3$
$0.4 > a \geq 0.3$	$w = 0.25$
$0.3 > a \geq 0.2$	$w = 0.2$

Table 3. *Cont.*

$a = \lvert x_{best}(t) - x_i(t) \rvert$	The Inertia Weight (w) in Equation (5)
$0.2 > a \geq 0.1$	$w = 0.15$
$0.1 > a \geq 0$	$w = 0.1$

4.4. MCSO with Fixed Initial Tracking Voltage Combined with Tracking Pace Adjusted by the Slope of P-V Curve and Inertia Weight

The use of distance $\lvert x_{best}(t) - x_i(t) \rvert$ to determine the achievement of GMPP tracking was not sufficient because it was possible that the location with the current optimal fitness was the LMPP instead of the GMPP. Therefore, to increase the tracking speed and determine whether the GMPP instead of the LMPP was tracked more accurately, MCSO is proposed in this paper. In addition to fixing the initial tracking voltage at 0.8 V_{mp}, it is combined with the slope of the P-V curve and the inertia weight at the same time to adjust the tracking pace. This tracking method can help to determine the status of the current work point more precisely; at the same time, the tracking pace can be increased by combining multiple parameters, which reduces the oscillation amplitude and enhances the tracking efficiency.

5. Design of MPPT Controlling Converter

In this work, we present an improved version of CSO, which turned out to outperform the original version in terms of GMPP tracking performance.

Figure 5 displays the architecture of MPPT for MCSO. The architecture mainly consists of a boost converter and MCSO. The boost converter was utilized [23,24] to adjust the output voltage of the PVMA, and the feedback of the PVMA voltage and current signals were measured by a differential amplifier. With MCSO, these signals are applied to adjust the next duty cycle through an iteration formula for MPPT.

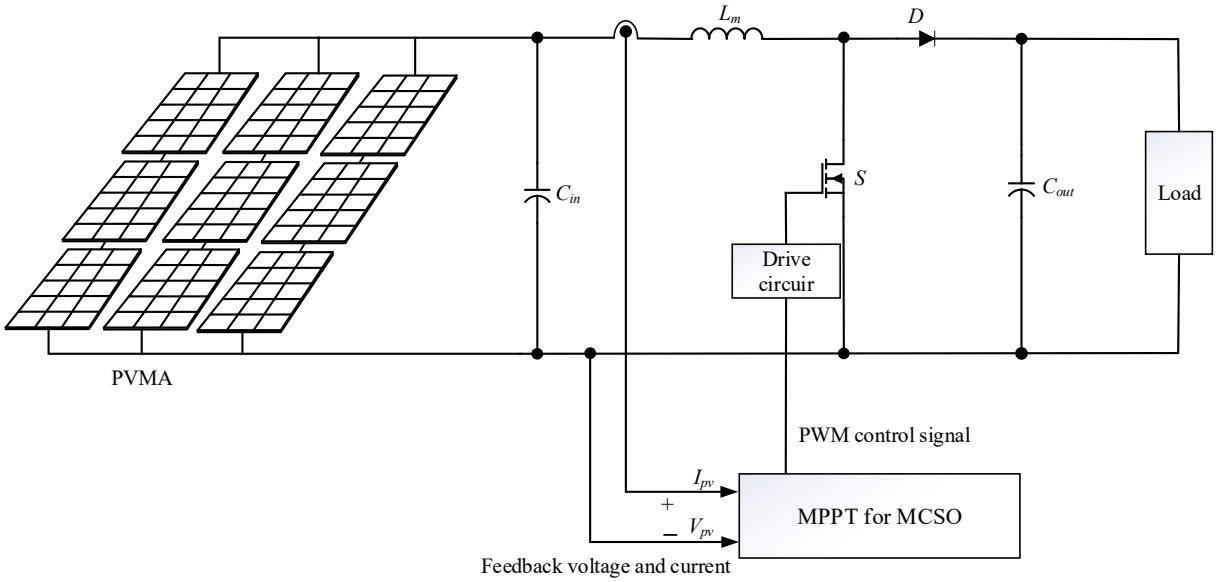

Figure 5. Architecture of MPPT for MCSO.

The circuit architecture of the boost converter consists of a storage inductor, a fast diode, a switch, and two filter capacitors. The relation between the output and input voltages of the boost converter is shown by Equation (6) [23]:

$$V_o = \frac{V_s}{1 - D} \tag{6}$$

where V_o is the output voltage, V_s is the input voltage, and D is the duty cycle. Since duty cycle D has a value between 0 and 1, the output voltage is always greater than or equal to the input voltage, so the converter is a boost converter. In this study, the switching frequency of the selected switch was 25 kHz. After calculation, the inductance, capacitance, and specifications of relevant components for the boost converter could be derived, as shown in Table 4 [23].

Table 4. Component specifications for boost converter [23].

Component	Specifications
Input capacitor, C_{in}	220 μF, withstand voltage: 400 V
Filter capacitance, C_{out}	470 μF, withstand voltage: 450 V
Energy storage inductance, L_m	1.67 mH, withstand voltage: 450 V
Fast diode, D (IQVD60E60A1)	Withstand voltage: 600 V, withstand current: 60 A
Switch, S (IREP460B)	Withstand voltage: 500 V, withstand current: 20 A

6. Simulated Results

Figure 5 shows the architecture of maximum power point tracking (MPPT) for cat swarm optimization (CSO) and modified cat swarm optimization (MCSO). In this paper, CSO and four types of MCSO are used to control the duty cycle of the boost converter, with the goal of tracking the maximum power point of the photovoltaic module array. The basic principle is to use the seeking and tracking modes in cat swarm optimization to find and track the maximum fitness (i.e., maximum PVMA output power) that was determined. The duty cycle of the boost converter's switch (S) is then adjusted via the pulse width modulation control circuit to ensure that the PVMA operates at the maximum power point voltage, allowing the PVMA to output the maximum power. MATLAB software was used to build the model of a four-series, three-parallel (total capacity: 239.1 W) PVMA assembled from single SWM20W photovoltaic modules. The solar irradiance of all 12 photovoltaic modules was suddenly reduced to half under different shading percentages at 0.1 s. Various proposed MCSO methods were utilized for the MPPT test, in which the tracking speed response and steady performance under various different tracking methods were compared. The status of different peak numbers based on the shading percentage of each test case and the corresponding P-V characteristic curves are shown in Table 5. The parameters for the conventional CSO and MCSO utilized in this paper are shown in Table 6.

Table 5. Peak numbers on P-V characteristic curve of 4-series, 3-parallel PVMA under 6 shading conditions.

Scenario	Peak Numbers on P-V Characteristic Curve	4-Series, 3-Parallel Shading %
1	Single-peak	(0% shading + 0% shading + 0% shading + 0% shading)// (0% shading + 0% shading + 0% shading + 0% shading)// (0% shading + 0% shading + 0% shading + 0% shading)
2	Double-peak (MPP at right)	(50% shading + 0% shading + 0% shading + 0% shading)// (0% shading + 0% shading + 0% shading + 0% shading)// (0% shading + 0% shading + 0% shading + 0% shading)

Table 5. *Cont.*

Scenario	Peak Numbers on P-V Characteristic Curve	4-Series, 3-Parallel Shading %
3	Triple-peak (MPP at right)	(0% shading + 80% shading + 0% shading + 100% shading)// (0% shading + 0% shading + 0% shading + 0% shading)// (0% shading + 0% shading + 0% shading + 0% shading)
4	Triple-peak (MPP at middle)	(0% shading + 100% shading + 0% shading + 50% shading)// (0% shading + 0% shading + 0% shading + 0% shading)// (0% shading + 0% shading + 0% shading + 0% shading)
5	Quadruple-peak (MPP at the second peak)	(0% shading + 30% shading + 60% shading + 90% shading)// (0% shading + 30% shading + 60% shading + 90% shading)// (0% shading + 30% shading + 60% shading + 90% shading)
6	Quadruple-peak (MPP at the third peak)	(30% shading + 50% shading + 80% shading + 0% shading)// (30% shading + 50% shading + 80% shading + 0% shading)// (30% shading + 50% shading + 80% shading + 0% shading)

Note: + indicates series and // indicates parallel.

Table 6. Parameters for conventional CSO and MCSO.

Parameter	Conventional	Modified
Maximum iteration number (t)	30	
Random number (r)	[0~1]	
Inertia weight (w)	Zero usage w	[0.1~0.4]
Speed coefficient (c)	1.4	[1.0~1.4]
SRD	0.2%	

(1) Test of Case 1

Figure 6 shows the P-V characteristic curves of the PVMA in case 1 under solar irradiances of 1000 and 500 W/m^2 and zero shading, with the MPP at 239.1 and 121.1 W, respectively. Figure 7 shows the simulation results of the conventional CSO and four MCSO methods proposed in this paper. From the figure, it can be seen that under a solar irradiance change from 1000 W/m^2 to 500 W/m^2 and back to 1000 W/m^2 for all methods, only the conventional CSO could not track the GMPP when the solar irradiance suddenly changed to 500 W/m^2, and the maximum iteration number (t) was set as 30 times, while all four proposed MCSO methods could track the GMPP. Although the conventional CSO could track the GMPP at a solar irradiance of 1000 W/m^2, it could clearly be seen that the oscillation amplitude was greater compared to the four modified methods. Among them, the MCSO with the initial tracking voltage fixed at 0.8 times the MPP voltage (0.8 V_{mp}) under STC combined with a tracking pace adjusted with the slope of the P-V curve and inertia weight provided the optimal tracking speed response and steady performance.

(2) Test of Case 2

Figure 8 shows the P-V characteristic curves of the PVMA in case 2 at solar irradiances of 1000 and 500 W/m^2 with a single module under 50% shading, where the true MPP was at 201.7 and 102.1 W, respectively, and the GMPP was to the right. Figure 9 shows the simulation results for MPPT with the conventional CSO and four proposed MCSO methods. From the figure, it can be seen that under a solar irradiance change from 1000 W/m^2 to 500 W/m^2 and back to 1000 W/m^2, all five tracking methods could track the GMPP successfully. Although all five tracking methods were stuck with an LMPP of 187.4 W, the MCSO with an initial tracking voltage fixed at 0.8 V_{mp} combined with pace adjusted with the slope of the P-V curve and inertia weight could escape from the LMPP swiftly. The other methods could also escape but required a longer duration, and the oscillation amplitude was greater. In view of this, the MSCO proposed in this paper with the initial tracking voltage fixed at 0.8 V_{mp} combined with pace adjusted with the slope of the P-V curve and inertia weight provided an optimal tracking speed response, and the oscillation

amplitude after tracking the GMPP was lower compared to the other methods; hence, the steady performance was also better.

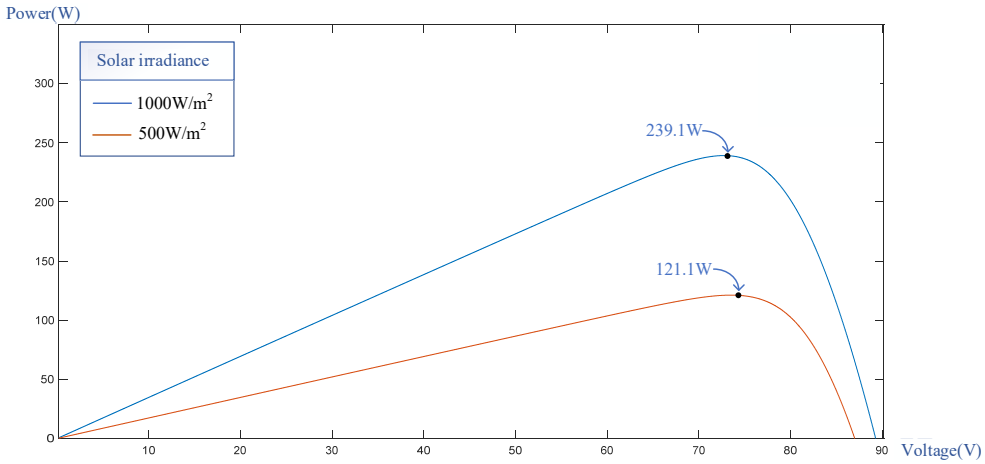

Figure 6. P-V characteristic curve for case 1.

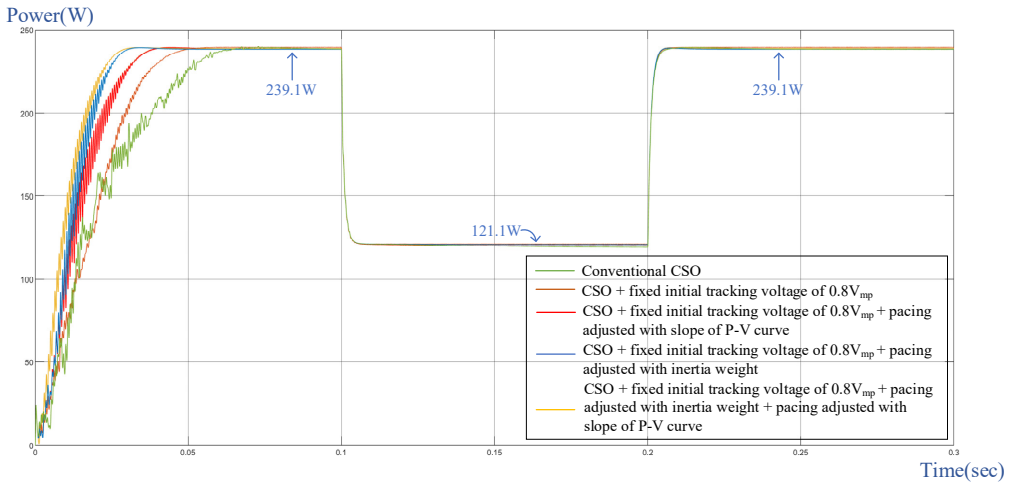

Figure 7. Simulation results for case 1: MPPT with conventional CSO and four modified methods under solar irradiance change from 1000 to 500 W/m^2 and back to 1000 W/m^2.

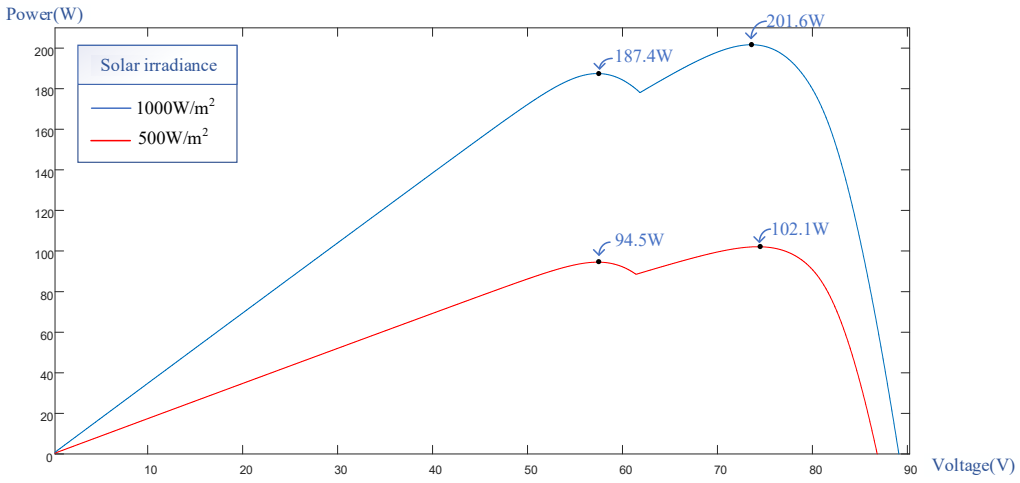

Figure 8. P-V characteristic curve for case 2.

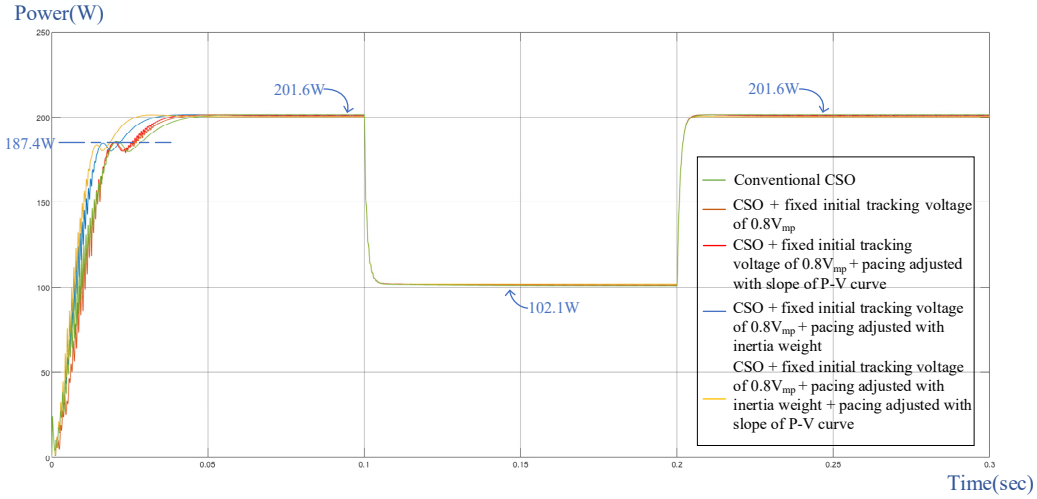

Figure 9. Simulation results for case 2: MPPT with conventional CSO and four modified methods under solar irradiance change from 1000 to 500 W/m^2 and back to 1000 W/m^2.

(3) Test of Case 3

Figure 10 shows the P-V characteristic curves of PVMA in case 3 at solar irradiances of 1000 and 500 W/m^2 with two modules under 80% and 100% shading, where three peaks appeared with true MPP at 159.4 and 80.7 W, respectively, and the GMPP was at the far right. Figure 11 shows the simulation results for MPPT with the conventional CSO and four proposed MCSO methods. From the figure, it can be seen that under a solar irradiance change from 1000 to 500 W/m^2 and back to 1000 W/m^2, although all five tracking methods could track the GMPP successfully, each was stuck with an LMPP at 121.7 and 154.8 W. Even though all five tracking methods could track to the GMPP eventually, it could be clearly observed that the conventional CSO required a longer duration, and the oscillation amplitude during the tracking process was greater. In view of this, the proposed MSCO with an initial tracking voltage fixed at 0.8 V_{mp} combined with pace adjusted with the slope of the P-V curve and inertia weight not only provided the fastest tracking speed response, but the oscillation amplitude near the GMPP was lower compared to the other methods.

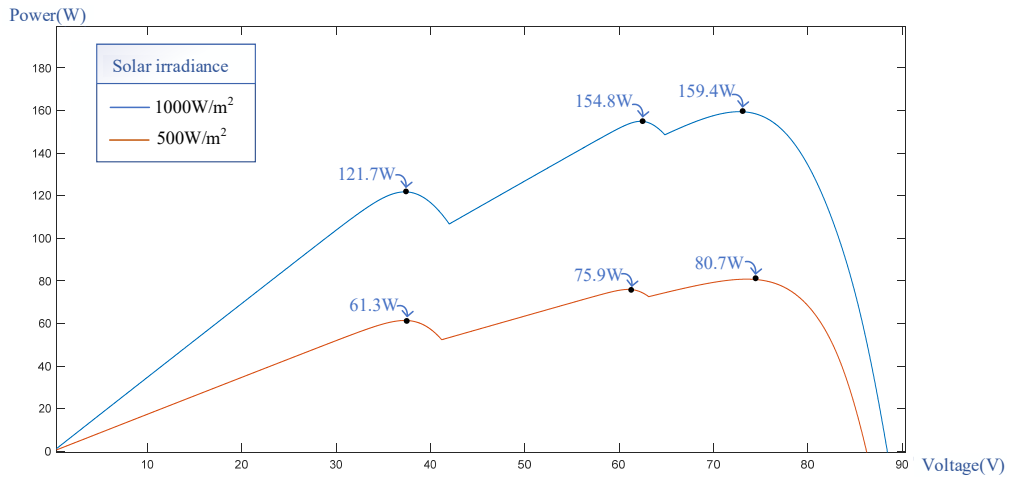

Figure 10. P-V characteristic curve for case 3.

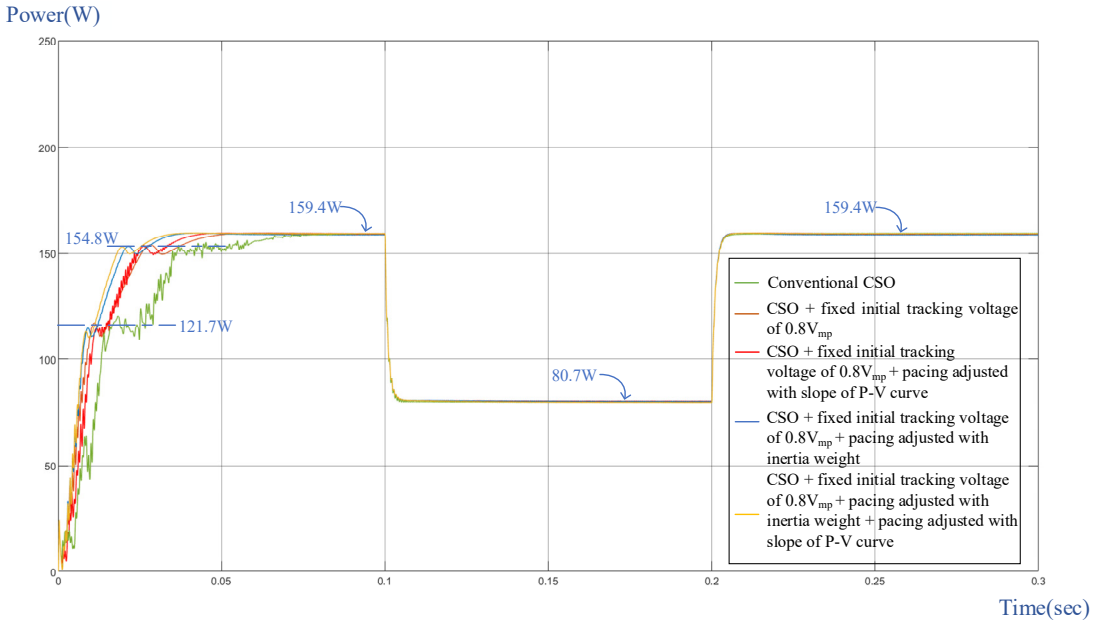

Figure 11. Simulation results for case 3: MPPT with conventional CSO and four modified methods under solar irradiance change from 1000 to 500 W/m^2 and back to 1000 W/m^2.

(4) Test of Case 4

Figure 12 shows the P-V characteristic curves of the PVMA in case 4 at solar irradiances of 1000 and 500 W/m^2 with two modules under 100% and 50% shading, where three peaks appeared with true MPP at 170.2 and 84.4 W, respectively, and the GMPP was in the middle. Figure 13 shows the simulation results for MPPT with the conventional CSO and four proposed MCSO methods. From the figure, it can be seen that under a solar irradiance change from 1000 to 500 W/m^2 and back to 1000 W/m^2, each method was stuck with an LMPP at 121.7 W. The four modified methods could escape from the stuck point swiftly and track the GMPP successfully. The conventional CSO under a solar irradiance of 1000 W/m^2 could not track the GMPP successfully within the set of 30 iterations. Although the four proposed tracking methods could track the GMPP successfully, the MCSO with the initial tracking voltage fixed at 0.8 V_{mp} combined with pace adjusted with the slope of the P-V curve and inertia weight provided the fastest tracking speed response, and the oscillation amplitude near the MPP was minor. Therefore, the power generation efficiency of the PVMA could be enhanced.

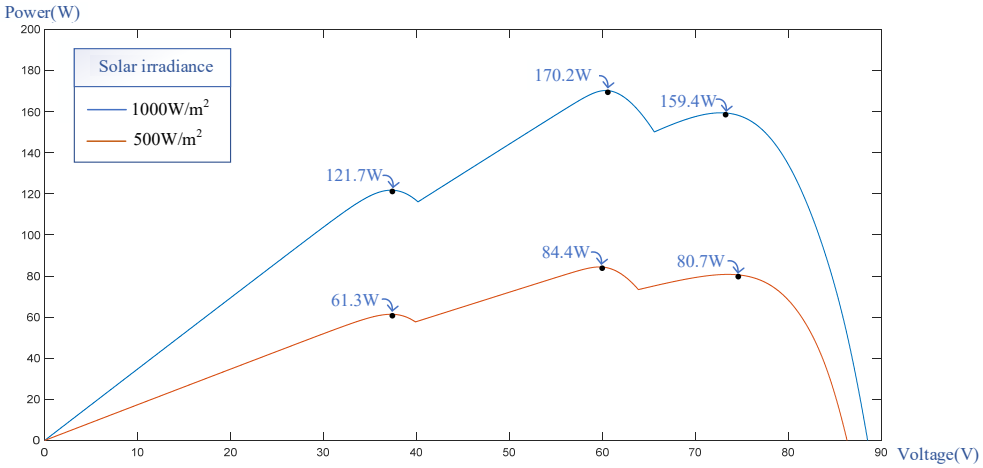

Figure 12. P-V characteristic curve for case 4.

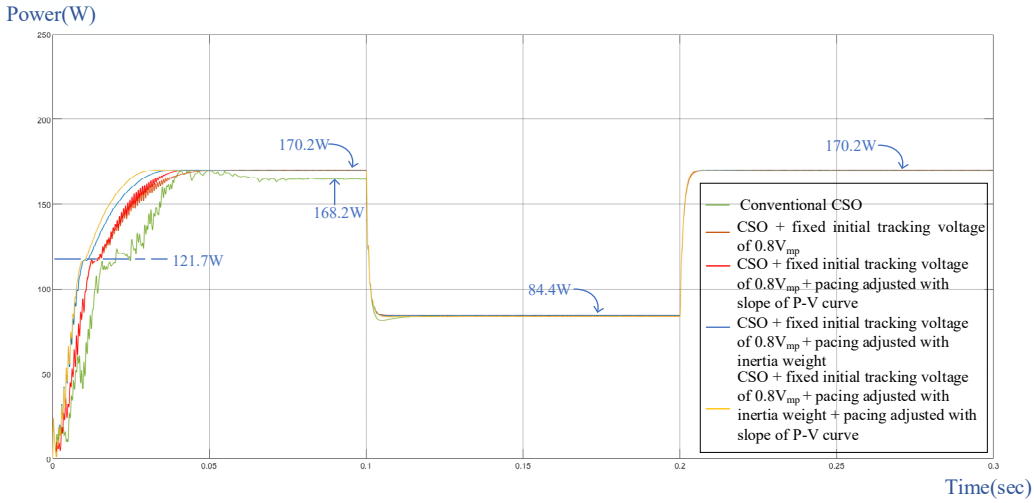

Figure 13. Simulation results for case 4: MPPT with conventional CSO and four modified methods under solar irradiance change from 1000 to 500 W/m^2 and back to 1000 W/m^2.

(5) Test of Case 5

Figure 14 shows the P-V characteristic curves of the PVMA in case 5 at solar irradiances of 1000 and 500 W/m^2 with nine modules under 30%, 60%, and 90% shading, where four peaks appeared with true MPP at 85.8 and 42.9 W, respectively, and the GMPP was at the second peak from the left. Figure 15 shows the simulation results for MPPT with the conventional CSO and four proposed MCSO methods. From the figure, it can be seen that under a solar irradiance change from 1000 to 500 W/m^2 and back to 1000 W/m^2, only the conventional CSO under a solar irradiance of 1000 W/m^2 could not track the GMPP. Although all four modified tracking methods proposed in this paper were stuck with an LMPP at 51.9 W, they could escape from the LMPP swiftly and track the GMPP successfully. Among them, the MCSO with the initial tracking voltage fixed at 0.8 V_{mp} combined with pace adjusted with the slope of the P-V curve and inertia weight could escape from the LMPP (51.9 W) the fastest. Therefore, this modified method provided optimal tracking speed response and steady performance.

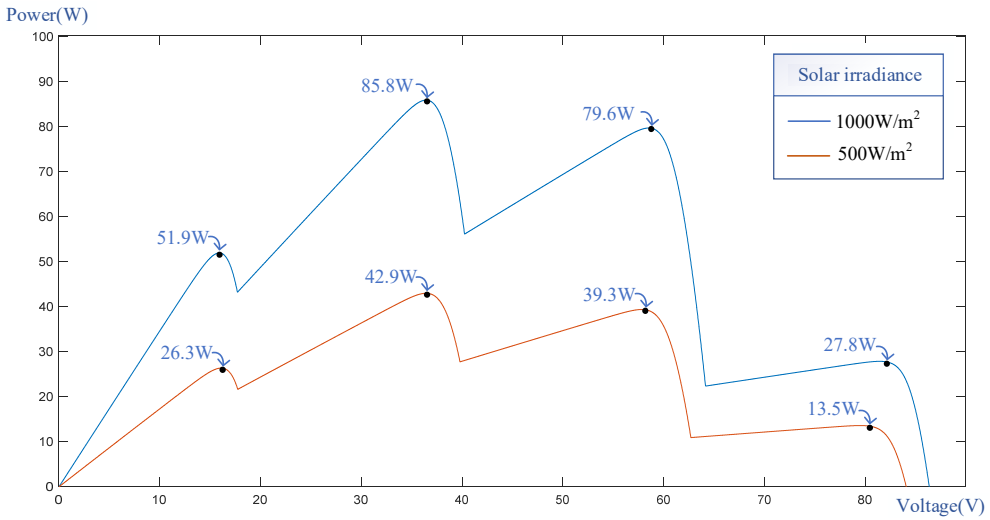

Figure 14. P-V characteristic curve for case 5.

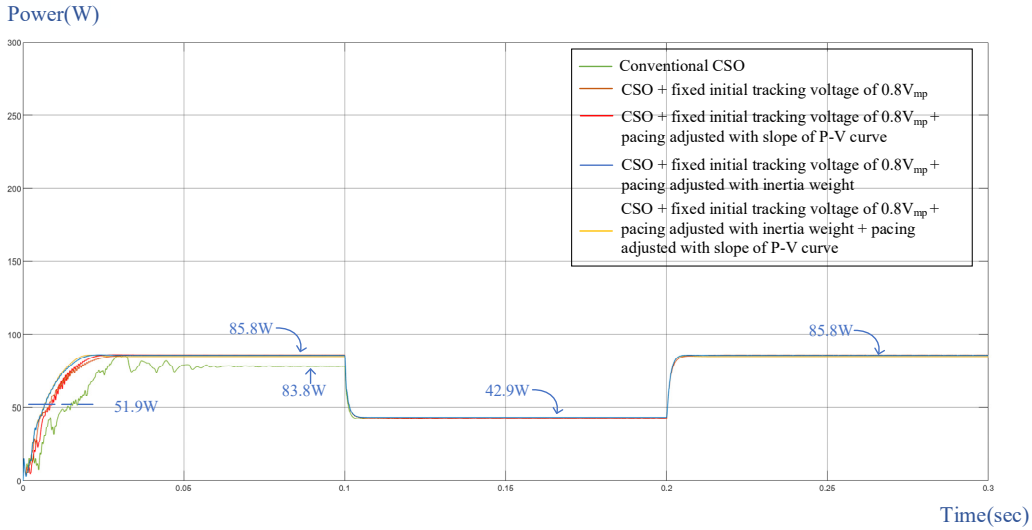

Figure 15. Simulation results for case 5: MPPT with conventional CSO and four modified methods under solar irradiance change from 1000 to 500 W/m^2 and back to 1000 W/m^2.

(6) Test of Case 6

Figure 16 shows the P-V characteristic curves of the PVMA in case 6 at solar irradiances of 1000 and 500 W/m^2 with nine modules under 30%, 50%, and 80% shading, where four peaks appeared with true MPP at 98.2 and 48.7 W, respectively, and the GMPP was at the third peak from the left. Figure 17 shows the simulation results for MPPT with the conventional CSO and four proposed MCSO methods. From the figure, it can be seen that under a solar irradiance change from 1000 to 500 W/m^2 and back to 1000 W/m^2, only the conventional CSO under a solar irradiance of 1000 W/m^2 could not track the GMPP. Although all four modified tracking methods proposed in this paper were stuck with an LMPP at 51.9 and 85.8 W, they could escape swiftly and track the GMPP successfully under the two solar irradiance conditions. Among them, the MCSO with the initial tracking voltage fixed at 0.8 V_{mp} combined with pace adjusted with the slope of the P-V curve and inertia weight provided optimal tracking speed response and steady performance.

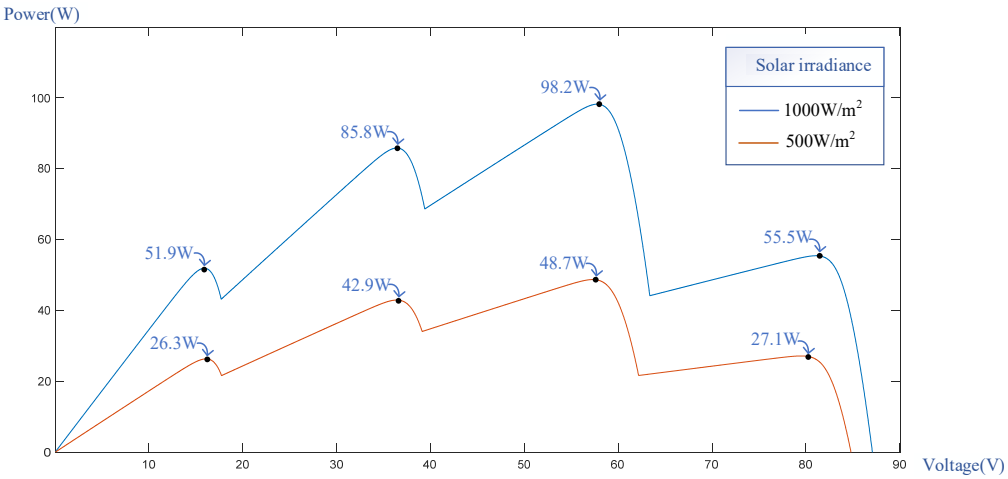

Figure 16. P-V characteristic curve simulation for case 6.

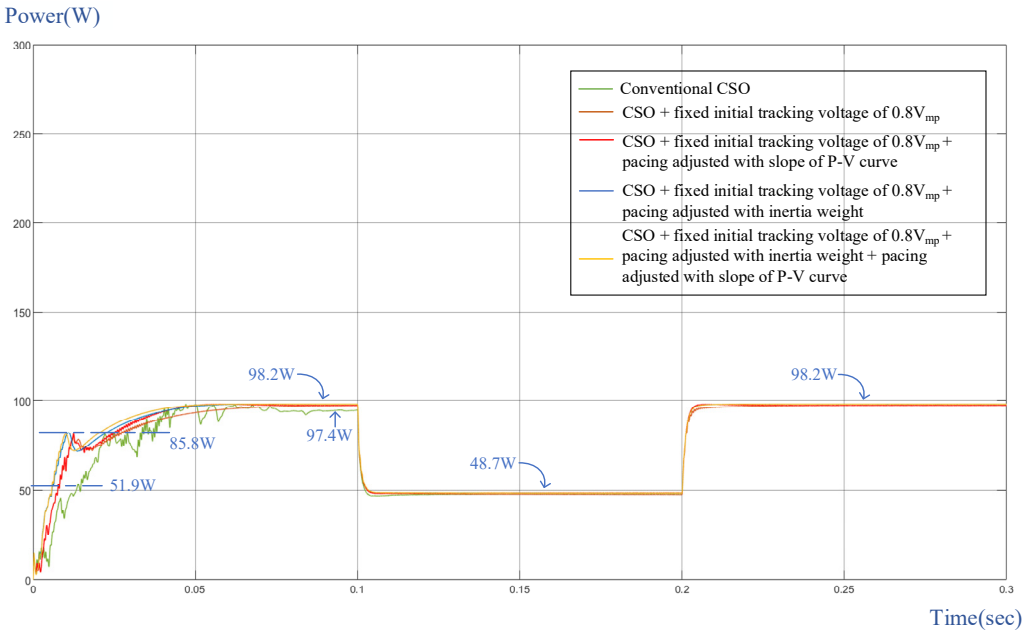

Figure 17. Simulation results for case 6: MPPT with conventional CSO and four modified methods under solar irradiance change from 1000 to 500 W/m^2 and back to 1000 W/m^2.

In cases 4, 5, and 6, the conventional cat swarm optimization (CSO) method failed to locate the global maximum point. This is because the maximum number of iterations for each tracking method was set to 30 in this study. As a result, the three cases using conventional cat swarm optimization were unable to track the global maximum power point within the limit of 30 iterations. However, as the solar exposure decreased from 1000 W/m^2 to 500 W/m^2, the maximum power point voltage did not change significantly because the shading conditions did not change. The previous tracking did not capture the global maximum power point, but it was close. As a result, tracking the global power point under 500 W/m^2 solar exposure took only a few iterations.

Tables 7 and 8 show comparisons of tracking time and oscillation amplitude when performing maximum power point tracking at the beginning of tracking for the six test cases using conventional cat swarm optimization (CSO) and four types of modified cat swarm optimization (MCSO). The tables show that, under various test conditions, the CSO with fixed initial tracking voltage combined with tracking pace adjusted by the slope of the P-V curve and inertia weight not only tracked the global maximum power point faster but also had a lower oscillation amplitude.

Table 7. Tracking speed comparison of six cases.

Case	Number of Peaks on P-V Curve	Tracking Speed				
		Conventional CSO Algorithm	CSO with Fixed Initial Tracking Voltage	CSO with Fixed Initial Tracking Voltage Combined with Tracking Pace Adjusted with Slope of P-V Curve	CSO with Fixed Initial Tracking Voltage Combined with Tracking Pace Adjusted by Inertia Weight	CSO with Fixed Initial Tracking Voltage Combined with Tacking Pace Adjusted by Slope of P-V Curve and Inertia Weight
1	Single peak	0.077 s	0.05 s	0.048 s	0.042 s	0.038 s
2	Double peak (MPP at right)	0.061 s	0.051 s	0.049 s	0.003 s	0.028 s

Table 7. *Cont.*

Case	Number of Peaks on P-V Curve	Tracking Speed				
		Conventional CSO Algorithm	CSO with Fixed Initial Tracking Voltage	CSO with Fixed Initial Tracking Voltage Combined with Tracking Pace Adjusted with Slope of P-V Curve	CSO with Fixed Initial Tracking Voltage Combined with Tracking Pace Adjusted by Inertia Weight	CSO with Fixed Initial Tracking Voltage Combined with Tacking Pace Adjusted by Slope of P-V Curve and Inertia Weight
3	Triple peak (MPP at right)	0.082 s	0.059 s	0.056 s	0.04 s	0.039 s
4	Triple peak (MPP at middle)	Fail	0.058 s	0.055 s	0.043 s	0.038 s
5	Quadruple peak (MPP at second peak)	Fail	0.037 s	0.028 s	0.023 s	0.02 s
6	Quadruple peak (MPP at third peak)	Fail	0.061 s	0.057 s	0.056 s	0.054 s

Table 8. Amplitude oscillation comparison of six cases using five MPPT methods.

Case	Number of Peaks on P-V Curve	Maximum Oscillation Amplitude				
		Conventional CSO Algorithm	CSO with Fixed Initial Tracking Voltage	CSO with Fixed Initial Tracking Voltage Combined with Tracking Pace Adjusted with Slope of P-V Curve	CSO with Fixed Initial Tracking Voltage Combined with Tracking Pace Adjusted by Inertia Weight	CSO with Fixed Initial Tracking Voltage Combined with Tacking Pace Adjusted by Slope of P-V Curve and Inertia Weight
1	Single peak	30 W	21 W	11 W	12 W	12 W
2	Double peak (MPP at right)	18 W	17 W	13 W	14 W	13 W
3	Triple peak (MPP at right)	30 W	10 W	9 W	12 W	11 W
4	Triple peak (MPP at middle)	17 W	10 W	8 W	10 W	5 W
5	Quadruple peak (MPP at second peak)	18 W	8 W	10 W	10 W	7 W
6	Quadruple peak (MPP at third peak)	21 W	10 W	12 W	10 W	6 W

7. Conclusions

The main purpose of this study was to improve the performance of conventional CSO in terms of MPPT so that it could also track the GMPP swiftly with a PVMA under different shading percentages and sudden changes in solar irradiance. We set the initial tracking voltage at 0.8 times the MPP voltage under STC and divided the output P-V characteristic curve of the PVMA into six slope intervals, which were utilized to adjust the tracking pace in the iteration formula, and the tracking pace was adjusted with the inertia weight as the learning rate. In addition, MCSO could provide a better tracking speed response and steady performance during MPPT.

In this paper, four MCSO methods are proposed: MCSO with a fixed initial traction voltage at 0.8 V_{mp}, MCSO with a fixed initial traction voltage at 0.8 V_{mp} combined with pace adjusted with the slope of P-V curve, MCSO with a fixed initial traction voltage at 0.8 V_{mp} combined with pace adjusted with the inertia weight, and MCSO with the initial tracking voltage fixed at 0.8 V_{mp} combined with pace adjusted with the slope of P-V curve and inertia weight. The simulation results show that these modified methods provided a better tracking speed response and steady performance compared to the conventional CSO. Among the four modified methods, MCSO with the initial tracking voltage fixed at 0.8 V_{mp} combined with pace adjusted with the slope of P-V curve and inertia weight provided a better tracking speed response and steady performance compared to the conventional CSO and the other three modified methods. Through the simulation results, it

was also proven that, under a sudden change in solar irradiance on a specific day, all four MCSO methods proposed in this paper could track the GMPP swiftly. Among them, MCSO with the initial tracking voltage fixed at 0.8 V_{mp} combined with pace adjusted with the slope of P-V curve and the inertia weight provided the optimal tracking speed response. After tracking the MPP, it could also reduce the back-and-forth tracking of the oscillation amplitude. Therefore, the power loss was decreased and the power generation efficiency of the PVMA was enhanced.

Author Contributions: K.-H.C. managed the project and completed the modified cat swarm optimization algorithm for the maximum power point tracking of PV module arrays. K.-H.C. also planned the project and wrote, edited, and reviewed the manuscript. T.B.-N.N. completed the formal analysis of the maximum power point tracking algorithm. T.B.-N.N. is also responsible for the software program and validating the simulation results. All authors have read and agreed to the published version of the manuscript.

Funding: The authors gratefully acknowledge the support for this project and funding from the National Science and Technology Council, Taiwan, under grant number NSTC 112-2221-E-167-002.

Institutional Review Board Statement: Not applicable.

Informed Consent Statement: Not applicable.

Data Availability Statement: Data is contained within the article.

Conflicts of Interest: The authors of the manuscript declare no conflicts of interest.

References

1. Akhtar, I.; Kirmani, S.; Jameel, M.; Alam, F. Feasibility Analysis of Solar Technology Implementation in Restructured Power Sector with Reduced Carbon Footprints. *IEEE Access* **2021**, *9*, 30306–30320. [CrossRef]
2. Infield, D.; Freris, L. *Renewable Energy in Power Systems*; John Wiley & Sons: Hoboken, NJ, USA, 2020; ISBN 1118649931.
3. Nguyen, T.B.N.; Chao, K.H. Fast Maximum Power Tracking for Photovoltaic Module Array Using Only Voltage and Current Sensors. *Sens. Mater.* **2023**, *35*, 2619–2635.
4. Baba, A.O.; Liu, G.; Chen, X. Classification and Evaluation Review of Maximum Power Point Tracking Methods. *Sustain. Futures* **2020**, *2*, 100020. [CrossRef]
5. Bhukya, L.; Kedika, N.R.; Salkuti, S.R. Enhanced Maximum Power Point Techniques for Solar Photovoltaic System under Uniform Insolation and Partial Shading Conditions: A Review. *Algorithms* **2022**, *15*, 365. [CrossRef]
6. Hanzaei, S.H.; Gorji, S.A.; Ektesabi, M. A Scheme-based Review of MPPT Techniques with Respect to Input Variables Including Solar Irradiance and PV Arrays' Temperature. *IEEE Access* **2020**, *8*, 182229–182239. [CrossRef]
7. Alrubaie, A.J.; Al-Khaykan, A.; Malik, R.; Talib, S.H.; Mousa, M.I.; Kadhim, A.M. Review on MPPT Techniques in Solar System. In Proceedings of the 2022 8th International Engineering Conference on Sustainable Technology and Development (IEC), Erbil, Iraq, 23–24 February 2022; pp. 123–128.
8. Díaz Martínez, D.; Trujillo Codorniu, R.; Giral, R.; Vázquez Seisdedos, L. Evaluation of Particle Swarm Optimization Techniques Applied to Maximum Power Point Tracking in Photovoltaic Systems. *Int. J. Circuit Theory Appl.* **2021**, *49*, 1849–1867. [CrossRef]
9. Szemes, P.T.; Melhem, M. Analyzing and Modeling PV with "P&O" MPPT Algorithm by MATLAB/SIMULINK. In Proceedings of the 3rd International Symposium on Small-Scale Intelligent Manufacturing Systems (SIMS), Gjovik, Norway, 10–12 June 2020; pp. 1–6.
10. Saber, H.; Bendaouad, A.E.; Rahmani, L.; Radjeai, H. A Comparative Study of the FLC, INC and P&O Methods of the MPPT Algorithm for a PV System. In Proceedings of the 19th International Multi-Conference on Systems, Signals & Devices (SSD), Sétif, Algeria, 6–10 May 2022; pp. 2010–2015.
11. Fan, Z.; Li, S.; Cheng, H.; Liu, L. Perturb and Observe MPPT Algorithm of Photovoltaic System: A Review. In Proceedings of the 33rd Chinese Control and Decision Conference (CCDC), Kunming, China, 22–24 May 2021; pp. 1413–1418.
12. Zhou, C.G.; Huang, L.; Ling, Z.X.; Cui, Y.B. Research on MPPT Control Strategy of Photovoltaic Cells under Multi-peak. *Energy Rep.* **2021**, *7*, 283–292. [CrossRef]
13. Yang, B.; Zhu, T.; Wang, J.; Shu, H.; Yu, T.; Zhang, X.; Yao, W.; Sun, L. Comprehensive Overview of Maximum Power Point Tracking Algorithms of PV Systems under Partial Shading Condition. *J. Clean. Prod.* **2020**, *268*, 121983. [CrossRef]
14. Javed, S.; Ishaque, K. A Comprehensive Analyses with New Findings of Different PSO Variants for MPPT Problem under Partial Shading. *Ain Shams Eng. J.* **2022**, *13*, 101680. [CrossRef]
15. Huang, Y.P.; Huang, M.Y.; Ye, C.E. A Fusion Firefly Algorithm with Simplified Propagation for Photovoltaic MPPT under Partial Shading Conditions. *IEEE Trans. Sust. Energy* **2020**, *11*, 2641–2652. [CrossRef]

16. Li, C.C.; Sun, C.Y.; Li, S.Q.; Zhang, Y.Y. An Integrated MPPT Control Strategy Using Circle Search-firefly Algorithm (CSFA) for Photovoltaic System. In Proceedings of the 4th International Conference on Smart Power & Internet Energy Systems (SPIES), Beijing, China, 9–12 December 2022; pp. 1945–1949.
17. Chao, K.H.; Zhang, S.W. An Maximum Power Point Tracker of Photovoltaic Module Arrays Based on Improved Firefly Algorithm. *Sustainability* **2023**, *15*, 8550. [CrossRef]
18. Millah, I.S.; Chang, P.C.; Teshome, D.F.; Subroto, R.K.; Lian, K.L.; Lin, J.-F. An Enhanced Grey Wolf Optimization Algorithm for Photovoltaic Maximum Power Point Tracking Control under Partial Shading Conditions. *IEEE Open J. Ind. Electron. Soc.* **2022**, *3*, 392–408. [CrossRef]
19. Huang, K.H.; Chao, K.H.; Kuo, Y.P.; Chen, H.H. Maximum Power Point Tracking of PV Module Arrays Based on a Modified Gray Wolf Optimization Algorithm. *Energies* **2023**, *16*, 4329. [CrossRef]
20. González, C.; Restrepo, C.; Kouro, S.; Rodriguez, J. MPPT Algorithm Based on Artificial Bee Colony for PV System. *IEEE Access* **2021**, *9*, 43121–43133. [CrossRef]
21. Nagadurga, T.; Narasimham, P.; Vakula, V. Global Maximum Power Point Tracking of Solar Photovoltaic Strings under Partial Shading Conditions Using Cat Swarm Optimization Technique. *Sustainability* **2021**, *13*, 11106. [CrossRef]
22. SunWorld Datasheet. Available online: http://www.ecosolarpanel.com/ecosovhu/products/18569387_0_0_1.html (accessed on 31 October 2022).
23. Reddy, D.S. Review on power electronic boost converters. *Aust. J. Electr. Electron. Eng.* **2021**, *18*, 127–137. [CrossRef]
24. Zongo, O. Comparing the Performances of MPPT Techniques for DC-DC Boost Converter in a PV System. *Walailak J. Sci. Technol.* **2021**, *18*, 6500. [CrossRef]